Journal of Catalysis **211,** 173–182 (2002)
doi:10.1006/jcat.2002.3731

Hydrogen-Assisted 1,2-Dichloroethane Dechlorination Catalyzed by Pt–Sn/SiO_2: Effect of the Pt/Sn Atomic Ratio

William D. Rhodes,*,[1] Károly Lázár,† Vladimir I. Kovalchuk,* and Julie L. d'Itri*,[2]

*Department of Chemical Engineering, University of Pittsburgh, Pittsburgh, Pennsylvania 15261; and †Institute of Isotope and Surface Chemistry, Chemical Research Center, Hungarian Academy of Sciences Budapest, P.O.B. 77, H-1525, Hungary

Received March 7, 2002; revised June 12, 2002; accepted June 27, 2002

Silica-supported Pt and Pt–Sn catalysts for the hydrogen assisted 1,2-dichloroethane dechlorination have been investigated. The addition of Sn to Pt suppresses catalyst deactivation and dramatically alters product selectivity. While the main product of the reaction catalyzed by Pt and Pt–Sn with a Pt/Sn atomic ratio $\geq$1 is ethane, balanced by ethyl chloride, the catalysts with a Pt/Sn ratio $<$1 produce ethylene (up to 100% for Pt1Sn3/SiO_2; catalyst nomenclature is based on the metal atomic ratio) with ethane as a balance. *In situ* Mössbauer spectroscopic results show that a considerable fraction of Sn in ethylene-selective Pt1Sn3/SiO_2 and Pt1Sn2/SiO_2 and in unselective Pt1Sn1/SiO_2 catalysts forms Pt–Sn alloys, with the rest of the Sn present as Sn^{4+} and Sn^{2+}. There is only a Sn-rich Pt–Sn alloy in the Pt1Sn3/SiO_2 catalyst after reduction at 220°C while both Sn-rich and Pt-rich Pt–Sn alloy species are present in the Pt1Sn1/SiO_2 and Pt1Sn2/SiO_2. It is suggested that Sn-rich Pt–Sn alloys are responsible for the ethylene formation in the $CH_2ClCH_2Cl + H_2$ reaction. The different catalytic performance of Pt1Sn2/SiO_2 and Pt1Sn1/SiO_2 catalysts is explained by their different microstructures. In the ethylene-selective Pt1Sn2/SiO_2, the Sn-rich Pt–Sn alloy phase encompasses the Pt-rich one, forming a cherrylike structure, whereas in the unselective Pt1Sn1/SiO_2, both the Pt-rich and Sn-rich alloy phases are exposed to the reaction mixture.

Key Words: **hydrogen-assisted dechlorination; 1,2-dichloroethane; ethylene; SiO_2; platinum; tin; Mössbauer spectroscopy.**

INTRODUCTION

A number of investigations have been published on the dechlorination of saturated vicinal chlorohydrocarbons in the presence of H_2 to form olefins. Specifically, supported Pt–Cu (1–3), Pd–Ag (4–7), and Pt–Sn (8) catalysts were reported to catalyze the hydrogen-assisted dechlorination of 1,2-dichloroethane, 1,2-dichloropropane, and 1,2,3-trichloropropane to form ethylene, propylene, or allyl chloride with selectivities close to 100%. Despite the number of explanations suggested (9–11), the role of the nonnoble metal in enhancing the selectivity toward olefin is still a matter of debate.

For the Pt–Sn bimetallic catalyst, Sn plays an essential role in controlling activity, selectivity, and catalyst stability for many reactions of hydrocarbon conversion (9–12). For example, the addition of Sn to Pt alters the product distribution by inhibiting isomerization and hydrogenolysis pathways. Hence, the selectivity is increased toward dehydrogenation (13–17) or dehydrocyclization (9–12, 18–21). These trends have been rationalized in terms of Pt–Sn adsorption behavior, structure, and coking resistance properties (22–39). However, the exact nature of these bimetallic systems is still debated, partly because the Pt–Sn system forms five intermetallic compounds (40) and tin can exist in three oxidation states, Sn(0), Sn(II), and Sn(IV) (41). Thus, the particular reaction mixture may play a decisive role in the formation of the catalyst microstructure, favoring one or another active Pt–Sn species.

The objective of the present investigation was to obtain a molecular-level understanding of the chemistry associated with the hydrogen-assisted 1,2-dichloroethane dechlorination catalyzed by silica-supported Pt–Sn catalysts. As Sn is inactive in the reaction and Pt is completely unselective toward ethylene, a mixed Pt–Sn species would be responsible for the high ethylene selectivity of the Pt–Sn catalysts. To this end, *in situ* ^{119}Sn Mössbauer spectroscopy was employed to identify the Sn-containing species in a series of Pt–Sn catalysts. These results were linked to the reaction kinetics investigation and the Pt–Sn phases responsible for ethylene formation in the 1,2-dichloroethane dechlorination reaction were determined.

EXPERIMENTAL

Catalyst Preparation and Routine Characterization

Davisil™ grade 645 (60–100 mesh, 300 $m^2\ g^{-1}$ surface area, 150-Å average pore diameter, 1.15 $cm^3\ g^{-1}$ pore volume) silica gel (Aldrich, 99+%) was used as a support. The catalysts were prepared by pore volume coimpregnation of

[1] Present address: Westinghouse Savannah River Company, Bldg 773A, Aiken, SC 29808.

[2] To whom correspondence should be addressed. Fax: 412-624-9639. E-mail: jditri@pitt.edu.

0021-9517/02 $35.00

TABLE 1

Results of Routine Catalyst Characterization

Catalyst	Pt/Sn atomic ratio: In impregnating solution	Pt/Sn atomic ratio: In reduced catalyst	Pt loading[a] (wt%)	Sn loading[a] (wt%)	Pt dispersion (%)[b]
Pt/SiO_2	∞	∞	1.8	0	49
$Pt10Sn1/SiO_2$	3.3	10	1.6	0.1	34
$Pt2Sn1/SiO_2$	1	2.5	1.2	0.3	17
$Pt1Sn1/SiO_2$	0.3	0.9	0.6	0.4	25
$Pt1Sn2/SiO_2$	0.2	0.5	0.4	0.5	16
$Pt1Sn3/SiO_2$	0.1	0.3	0.3	0.6	26
Sn/SiO_2	0	0	0	0.8	N/A

[a] ICP–OES, Galbraith Labs.

[b] Based on irreversible CO uptake, $CO/Pt_{total} \times 100\%$.

the support with solutions of $H_2PtCl_6 \cdot 6H_2O$ (Alfa, 99.9%) and $SnCl_2 \cdot 2H_2O$ (Aldrich, 98%) in 1 N HCl. The slurry was equilibrated overnight before drying at ambient temperature and pressure for 72 h followed by further drying at 100°C for 2 h under vacuum (~5 Torr). Freshly impregnated solids exhibited a bright red or dark red color, indicative of mixed Pt–Sn chloride complexes (42, 43). As the catalysts were drying at ambient temperature, their color changed to light pink and then to brownish orange, characteristic of $PtCl_4$ after being dried in vacuum. A fraction of tin chloride sublimed from the catalysts during vacuum drying. The results of elemental analyses for Pt and Sn (ICP–OES, Galbraith Labs.) of the catalysts reduced at 220 and 350°C are shown in Table 1. The numbers were identical within measurement uncertainty for both reduction temperatures. The catalyst nomenclature is based on the metal atomic ratio. For example, $Pt1Sn2/SiO_2$ refers to a Pt/Sn atomic ratio of 1 : 2.

Carbon monoxide chemisorption measurements were conducted at 35°C with a volumetric sorption analyzer (Micromeritics® ASAP 2010). The adsorbate–metal ratio (Table 1) was determined from irreversibly adsorbed CO; the adsorption stoichiometry was assumed to be one. Prior to the CO chemisorption measurement, the catalyst was reduced in H_2 flow at 300°C for 2 h followed by reduction at 350°C for 1 h. Then it was evacuated at 350°C and cooled to the measurement temperature.

Kinetics Experiments

The dechlorination of CH_2ClCH_2Cl was conducted at ambient pressure in a stainless-steel flow reaction system connected to a quartz microreactor (10- or 20-mm i.d.) in which the catalyst was supported on a quartz frit. The reactor zone containing the catalyst was heated by an electric furnace. The temperature of the catalyst was measured and controlled with an accuracy of ±1°C with a temperature controller (Omega model CN2011). Gaseous reactants were metered with mass flow controllers (Brooks, 5850E) and mixed prior to entering the reactor. The liquid CH_2ClCH_2Cl (Sigma–Aldrich, 99.8%) was maintained at 0°C and metered into the reaction system via a saturator; He was the carrier gas. Saturation was confirmed by varying the flow rate of He through the saturator and quantifying the CH_2ClCH_2Cl in the gas phase by a gas chromatograph (GC) (Varian 3300 series).

The effluent from the reactor was analyzed online by GC and, when necessary, GC/MS to identify the reaction products. The GC was equipped with a 10-ft 60/80 Carbopack B/5% Fluorocol packed column (Supelco) and a flame ionization detector (FID) capable of detecting concentrations >1 ppm for all chlorocarbons and hydrocarbons involved in this study. The online HP GC/MS system consisted of a HP 5890 series II plus GC also equipped with a Fluorocol column connected to a HP 5972 mass-selective detector. Hydrogen chloride, a reaction product, was detected by GC/MS but was not quantified.

Prior to reaction, the catalyst was exposed to flowing He (Praxair, 99.999%, 30 ml min^{-1}) while it was heated from 30 to 130°C at the rate of 7°C min^{-1} and then held at 130°C for 60 min. Then the gas stream was switched to a mixture of H_2 (Praxair, 99.999%, 10 ml min^{-1}) and He (50 ml min^{-1}). Next, the catalyst was heated from 130°C to the reduction temperature (220 or 350°C) over a 30-min period and held at this temperature for 90 min. The catalyst was then quickly cooled in He (50 ml min^{-1}) to the reaction temperature.

For a typical dechlorination reaction, 0.1 g of catalyst was used and the total flow of reactant mixture through the reactor was 42 ml min^{-1}. The flow consisted of CH_2ClCH_2Cl (7300 ppm), H_2 (36,800 ppm), and He (balance). The reaction temperature was 200°C. The turnover frequency (TOF) values were based on CO chemisorption measurements. When comparing selectivities of the bimetallic catalysts, the catalyst mass and reactant mixture flow rate were adjusted to maintain the conversion at comparable levels (1.0–2.4%). However, in the case of Sn/SiO_2, no conversion was detected, even with 1 g of catalyst and a total reactant flow through the reactor of 3 ml min^{-1}.

Mössbauer Spectroscopy

^{119}Sn Mössbauer spectra were recorded at 77 K in an *in situ* cell (44) with a pellet supported by a thin Be plate. The pellet was made from a powdered catalyst sample (ca. 0.7 g) by pressing (100 MPa). Spectra were obtained for as-prepared samples, after reduction in a H_2 flow at 220°C and after another reduction of the same sample at 350°C (2 h, 10 ml min^{-1}, ambient pressure). The last spectrum for each sample was collected after exposure of the reduced catalyst to a flow of $CH_2ClCH_2Cl + H_2 + N_2$ (1 : 5 : 25, 13 ml min^{-1}, ambient pressure) at 200°C. The exposure period was adjusted to provide a quasi-steady-state catalyst's performance in the 1,2-dichloroethane dechlorination.

The cell was isolated after each step (e.g., sealed in the specific treatment gas) and cooled to the measurement temperature.

The constant acceleration Mössbauer spectra were collected with a KFKI spectrometer and a $Ba^{119m}SnO_3$ source (300 MBq). For fitting purposes, components of the Lorentzian line shape were assumed, and no isomer shift parameters were initially constrained. Successive iterations were applied to obtain a better fit to the experimentally generated data. The estimated accuracy of positional parameters is 0.03 mm s^{-1}. The isomer shift values are presented relative to SnO_2 (room temperature).

RESULTS

Kinetics Experiments

The kinetics results for catalysts reduced at 220°C are shown in Table 2. The monometallic Pt/SiO_2 and the bimetallic Pt–Sn/SiO_2 catalysts were active for 1,2-dichloroethane dechlorination; Sn/SiO_2 was inactive. The Pt/SiO_2 was permanently deactivated as the 1,2-dichloroethane conversion decreased by an order of magnitude during the first 100 h on stream (Fig. 1). In contrast, the conversion for the Sn-containing catalysts decreased by a factor of 2–3 during the first hour on stream and remained essentially constant thereafter. The sample with the highest Pt/Sn atomic ratio (Pt10Sn1/SiO_2) exhibited the highest steady-state turnover frequency (TOF) (Table 2). However, as the Pt/Sn ratio decreased, the TOFs of Pt–Sn catalysts gradually decreased to be an order of magnitude lower for the Pt1Sn3/SiO_2 than for the monometallic Pt.

The kinetics results show that the Sn content does not significantly influence product selectivity for the catalysts with a high Pt/Sn ratio (Table 2). For the Pt/SiO_2 and Pt–Sn/SiO_2 with Pt/Sn atomic ratios ≥ 1, the major and minor products were ethane and ethyl chloride, respectively. The Pt/SiO_2 exhibited a transient period (ca. 90 h on steam) wherein the selectivity toward ethyl chloride progressively increased from 9 to 18%, at the expense of ethane (Fig. 1). The dramatic difference occurred when the Pt/Sn atomic ratio becomes less than 1. Both the Pt1Sn2/SiO_2 and Pt1Sn3/SiO_2 do not catalyze 1,2-dichloroethane dechlorination toward monochloroethane; only ethane and ethylene form with steady-state ethylene selectivity at 86 and 96%, respectively (Table 2). The ethylene selectivity for these catalysts increased with TOS at the expense of ethane. The ethylene selectivity of Pt1Sn2/SiO_2 increased the most, from 34 to 86% during approximately 50 h on stream (Table 2, Fig. 2).

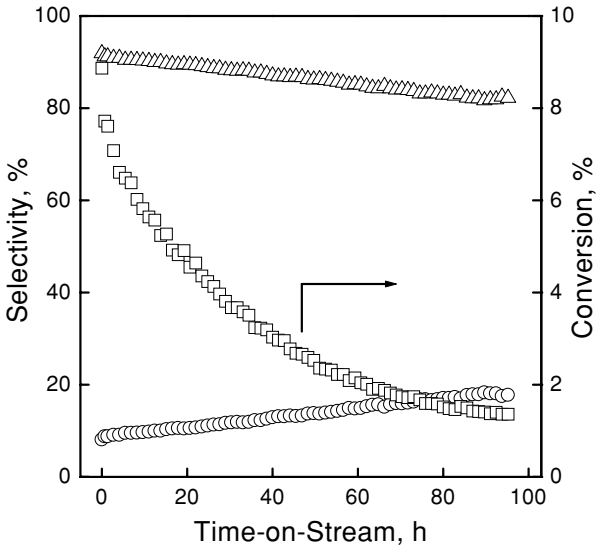

FIG. 1. Time on stream performance of Pt/SiO_2 reduced at 220°C: △, ethane; ○, ethyl chloride; □, conversion.

Increasing the reduction temperature from 220 to 350°C did not have a profound impact on the kinetics performance of the catalysts studied (Tables 2 and 3). The only significant effect was observed for the Pt1Sn2/SiO_2. The

TABLE 2

1,2-Dichloroethane Dechlorination Catalyzed by (Pt–Sn)/SiO_2 Reduced at 220°C

Catalyst	TOS for SS[a] (h)	Conversion[b] (%)	Initial selectivity[c] (mol%)			Steady-state selectivity (mol%)			TOF (10^4 s^{-1})
			C_2H_4	C_2H_6	C_2H_5Cl	C_2H_4	C_2H_6	C_2H_5Cl	
Pt	85	1.4	0	91	9	0	82	18	23.0
Pt10Sn1	19	1.7	0	91	9	0	89	11	66.0
Pt2Sn1	12	2.4	0	96	4	0	95	5	24.0
Pt1Sn1	2	1.8	0	95	5	0	96	4	6.8
Pt1Sn2	42	1.3	34	66	0	86	14	0	6.4
Pt1Sn3	8	1.0	87	13	0	96	4	0	4.0
Sn	N/A	0	N/A	N/A	N/A	N/A	N/A	N/A	0.0

[a] Time on stream to reach the steady-state catalyst's performance when the change in conversion was less than 0.1% and the change in product selectivity was less than 1% for 5 h.

[b] At steady state.

[c] After 0.7 h on stream.

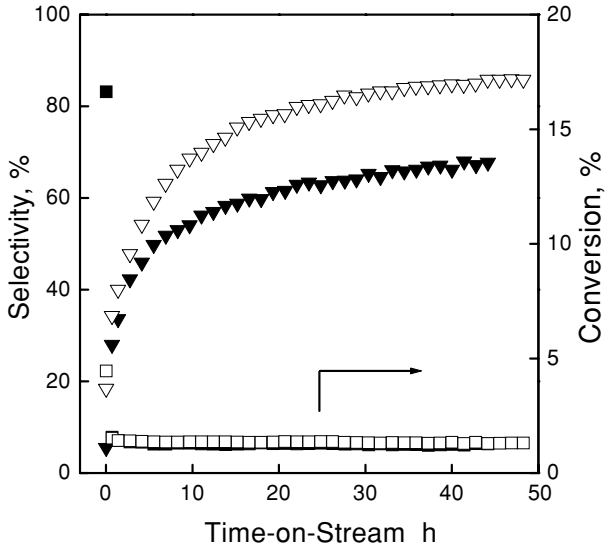

FIG. 2. Time on stream performance of Pt1Sn2/SiO_2: ▽, ethylene for the catalyst reduced at 220°C (balance is ethane); ▼, ethylene for the catalyst reduced at 350°C (balance is ethane); □, conversion for the catalyst reduced at 220°C; ■, conversion for the catalyst reduced at 350°C.

steady-state ethylene selectivity of the catalyst decreased from 86 to 68% as the reduction temperature was increased from 220 to 350°C (Tables 2 and 3, Fig. 2). For the Pt/SiO_2, Pt10Sn1/SiO_2, Pt2Sn1/SiO_2, and Pt1Sn1/SiO_2 catalysts, increasing the reduction temperature resulted in a somewhat longer transient period to attain steady-state conditions with essentially unchanged steady-state product selectivities.

^{119}Sn Mössbauer Spectroscopy

The ^{119}Sn Mössbauer study was performed for the Pt1Sn1/SiO_2, Pt1Sn2/SiO_2, and Pt1Sn3/SiO_2 catalysts, which showed dramatically different behavior in 1,2-dichloroethane dechlorination (Tables 2 and 3). The spectra are shown in Figs. 3–5. The parameters of the spectra are summarized in Table 4.

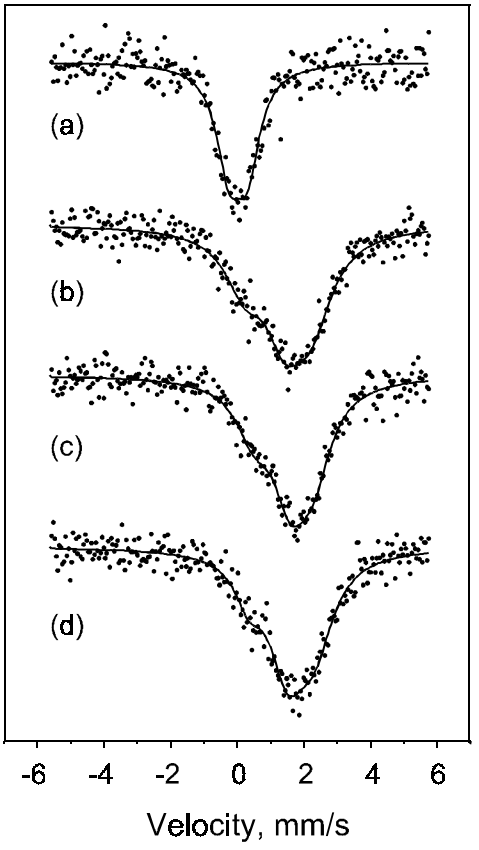

FIG. 3. Mössbauer spectra of Pt1Sn1/SiO_2: (a) as prepared; (b) sample (a) after reduction with H_2 at 220°C for 2 h; (c) sample (b) after reduction with H_2 at 350°C for 2 h; (d) sample (c) after exposure to a flow of $CH_2ClCH_2Cl + H_2 + N_2$ (1 : 5 : 25) at 200°C for 5 h.

Although the Sn precursor to prepare the catalysts was $SnCl_2$, the Mössbauer spectra of the as-prepared Pt–Sn

TABLE 3

1,2-Dichloroethane Dechlorination Catalyzed by (Pt–Sn)/SiO_2 Reduced at 350°C

Catalyst	TOS for SS[a] (h)	Conversion[b] (%)	Initial selectivity[c] (mol%)			Steady-state selectivity (mol%)			TOF (10^4 s^{-1})
			C_2H_4	C_2H_6	C_2H_5Cl	C_2H_4	C_2H_6	C_2H_5Cl	
Pt	89	1.3	0	91	9	0	83	17	22.0
Pt10Sn1	34	1.3	0	89	11	0	89	11	46.0
Pt2Sn1	14	2.3	0	94	6	0	95	5	22.0
Pt1Sn1	15	2.2	0	92	8	0	95	5	7.5
Pt1Sn2	39	1.3	28	72	0	68	32	0	6.1
Pt1Sn3	4	1.0	90	10	0	98	2	0	3.8
Sn	N/A	0	N/A	N/A	N/A	N/A	N/A	N/A	0.0

[a] Time on stream to reach the steady-state catalyst's performance when the change in conversion was less than 0.1% and the change in product selectivity was less than 1% for 5 h.

[b] At steady state.

[c] After 0.7 h on stream.

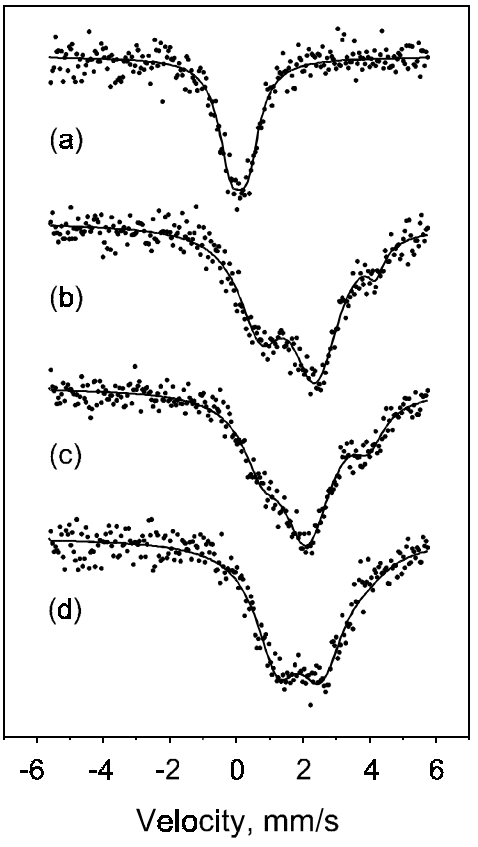

FIG. 4. Mössbauer spectra of Pt1Sn2/SiO_2: (a) as prepared; (b) sample (a) after reduction with H_2 at 220°C for 2 h; (c) sample (b) after reduction with H_2 at 350°C for 2 h; (d) sample (c) after exposure to a flow of $CH_2ClCH_2Cl + H_2 + N_2$ (1 : 5 : 25) at 200°C for 24 h.

samples consisted only of a quadrupole doublet with the splitting of 0.50–0.55 mm s^{-1} (Table 4). The isomer shift (IS) of the doublet varied from 0.01 to 0.11 mm s^{-1} depending on the catalyst. These parameters are characteristic of Sn(IV) with Cl and O ligands (45). Thus, the Sn(II) oxidized to Sn(IV) during storage of the catalysts, as could be expected from the chemistry of Sn(II) compounds (41).

The features of the Mössbauer spectra of the pretreated Pt–Sn samples suggest the presence of three forms of Sn, assigned to Sn(IV) species (IS = 0.21–0.54 mm s^{-1}), Sn(II) species (IS = 3.95–4.15 mm s^{-1}), and Pt–Sn alloy (IS = 1.11–2.53 mm s^{-1}) (18, 46–49), with a considerable fraction of tin alloyed with Pt (Table 4). The Sn(II) parameters were almost independent of the catalyst and the catalyst pretreatment and coincided with those for $SnCl_2$ (59). Similar to the as-prepared catalysts, the IS of Sn(IV) species in pretreated samples varied significantly, inferring changes in the species stoichiometry (45, 50). No QS was constrained for the Sn(IV) species at deconvolution of the spectra. The QS of $SnCl_4$ is zero (62), whereas that of SnO_2 is 0.5–0.7 mm s^{-1} (46, 47, 51), which is very close to the linewidth of the ^{119}Sn source (0.63 mm s^{-1} (50)). Thus, when the Sn(IV) band had a relatively low intensity (<20–30%), the QS parameter was unimportant because it did not increase the quality of the fit.

The broad line of the alloyed phase indicates that the Pt–Sn/SiO_2 catalysts contained several types of platinum–tin alloys. The Mössbauer spectra were fit to one and two alloy components and the fit with the higher confidence level was accepted. Accordingly, either one or two Pt–Sn components are distinguished in the present study: a platinum-rich component, PtSn(a), covering the IS range from 1.1 to 1.7 mm s^{-1}, and/or a tin-rich component, PtSn(b), from 1.8 to 2.5 mm s^{-1}. As a result, the isomer shift values were averaged within the designated PtSn(a) and PtSn(b) components, and compositional changes in the Pt–Sn alloy species were estimated from the mean IS value shift based on the proportionality of the IS and the Pt/Sn atomic ratio (49).

The changes in relative intensities (RI) of the spectral components corresponding to the different Sn species and in composition of Pt–Sn alloys for the Pt1Sn1/SiO_2, Pt1Sn2/SiO_2, and Pt1Sn3/SiO_2 catalysts resulting from different catalyst pretreatments are described below. The RIs do not strictly correspond to the concentrations because the probability of the Mössbauer effect (recoilless fraction) is

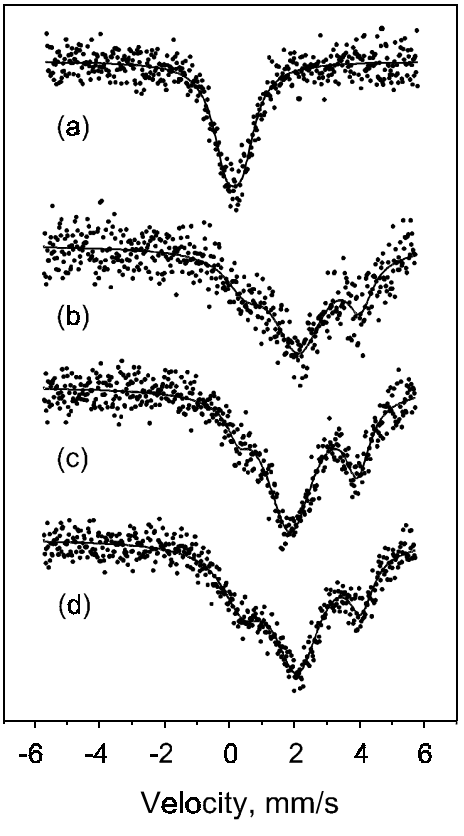

FIG. 5. Mössbauer spectra of Pt1Sn3/SiO_2: (a) as prepared; (b) sample (a) after reduction with H_2 at 220°C for 2 h; (c) sample (b) after reduction with H_2 at 350°C for 2 h; (d) sample (c) after exposure to a flow of $CH_2ClCH_2Cl + H_2 + N_2$ (1 : 5 : 25) at 200°C for 4 h.

TABLE 4

Parameters of Mössbauer Spectra of the Pt–Sn/SiO_2 Catalysts

Sample	Treatment[a]	Species[b]	IS[c] (mm s^{-1})	QS[d] (mm s^{-1})	FWHM[e]	RI[f] (%)	S_{tot}[g] (a.u.)
Pt1Sn1	As prepared	Sn^{4+}	0.01	0.55	0.92	100	1.00
	Reduced by	Sn^{4+}	0.21	—	1.40	20	1.41
	H_2 at 220°C	Pt–Sn(a)	1.48	—	1.65	52	
		Pt–Sn(b)	2.29	—	1.37	26	
	Reduced by	Sn^{4+}	0.45	—	1.17	15	1.42
	H_2 at 350°C	Pt–Sn(a)	1.64	—	1.57	63	
		Pt–Sn(b)	2.34	—	1.20	21	
	Exposed to	Sn^{4+}	0.31	—	0.84	9	1.33
	reaction mixture	Pt–Sn(a)	1.55	—	1.62	65	
	at 200°C	Pt–Sn(b)	2.36	—	1.27	26	
Pt1Sn2	As prepared	Sn^{4+}	0.07	0.50	0.89	100	1.00
	Reduced by	Sn^{4+}	0.54	—	1.31	24	1.54
	H_2 at 220°C	Pt–Sn(a)	1.39	—	1.64	21	
		Pt–Sn(b)	2.45	—	1.48	50	
		$SnCl_2$	4.15	—	0.74	5	
	Reduced by	Sn^{4+}	0.38	—	0.68	6	1.74
	H_2 at 350°C	Pt–Sn(a)	1.11	—	1.29	19	
		Pt–Sn(b)	2.16	—	1.69	64	
		$SnCl_2$	3.95	—	1.14	12	
	Exposed to	Pt–Sn(a)	1.22	—	1.59	43	1.42
	reaction mixture	Pt–Sn(b)	2.53	—	1.76	52	
	at 200°C	$SnCl_2$	3.96	—	1.58	5	
Pt1Sn3	As prepared	Sn^{4+}	0.11	0.50	0.97	100	1.00
	Reduced by	Sn^{4+}	0.52	—	1.37	15	1.41
	H_2 at 220°C	Pt–Sn(b)	2.19	—	1.89	69	
		$SnCl_2$	4.08	—	0.93	16	
	Reduced by	Sn^{4+}	0.47	—	1.26	15	1.47
	H_2 at 350°C	Pt–Sn(b_1)	1.81	—	1.27	50	
		Pt–Sn(b_2)	2.53	—	0.83	11	
		$SnCl_2$	3.98	—	1.03	25	
	Exposed to	Sn^{4+}	0.33	—	1.33	20	1.53
	reaction mixture	Pt–Sn(a)	1.19	—	1.02	6	
	at 200°C	Pt–Sn(b)	2.18	—	1.59	58	
		$SnCl_2$	4.09	—	0.96	16	

[a] All experiments for a given catalyst were performed with the same sample, which was treated *in situ* with H_2 first at 220°C for 2 h, then at 350°C for 2 h. Then it was exposed to the $CH_2Cl–CH_2Cl + H_2 + N_2$ (1 : 5 : 25) flow at 200°C for 5, 24, and 4 h for Pt1Sn1, Pt1Sn2, and Pt1Sn3, respectively.

[b] Pt–Sn(a), platinum-rich Pt–Sn alloys; Pt–Sn(b), tin-rich Pt–Sn alloys.

[c] Isomer shift relative to SnO_2.

[d] Quadrupole splitting.

[e] Full width at half maximum.

[f] Normalized relative intensity. Because the probability of the Mössbauer effect (recoilless fraction) is different for the various Sn species (50), the RIs do not strictly correspond to concentrations.

[g] The total spectral area related to the baseline, arbitrary units.

different for different Sn species (50, 52). In general, recoilless fractions for inorganic Sn(II) and Sn(IV) compounds are less than those for Pt–Sn alloys (52, 53). Thus, the relative concentrations of ionic Sn species based entirely on the RIs would be underestimated, whereas those of Pt–Sn alloy species would be overestimated.

Catalyst Pt1Sn1/SiO_2. The IS values of the two Pt–Sn alloy components fell within 1.48–1.64 and 2.29–2.36 mm s^{-1} and did not change significantly as a result of the reductions and reaction mixture treatment. These parameters are close to those of Pt_3Sn and $PtSn_4$ phases, respectively (49). Further, the relative intensity of the tin-rich Pt–Sn alloy was almost constant (21–26%); however, the RI of the platinum-rich Pt–Sn alloy increased from 52 to 65% through the course of the two reductions and reaction mixture treatment. This increase was at the expense of Sn(IV); its RI decreased from 20% for the sample reduced

at 220°C to 9% after exposure to the reaction mixture (Table 4).

Catalyst Pt1Sn2/SiO_2. For the tin-rich Pt–Sn alloy, the IS and RI values were similar after the reduction of the catalyst at 220°C and after exposure to the reaction mixture. The ISs of the alloy for these treatments exceeded that of $PtSn_4$ phase (2.29 mm s^{-1} (49)). The reduction at 350°C resulted in a lower IS (2.16 mm s^{-1}), corresponding to that of $PtSn_2$ phase (49) and higher RI (by ca. 13%). A similar trend was observed for the platinum-rich Pt–Sn alloy. Namely, increasing the reduction temperature from 220 to 350°C resulted in decreasing the IS from 1.39 to 1.11 mm s^{-1}, followed by increasing to 1.22 mm s^{-1} after exposure of the reduced catalyst to the reaction mixture. These IS values correspond to diluted solutions of Sn in Pt (49). In addition, exposure to the reaction mixture doubled the RI with respect to the levels measured after the two reductions (from ca. 20 to 43%). As the reduction temperature was increased from 220 to 350°C the RI of ionic tin decreased from 29 to 18% and decreased further to 5% after exposure to the reaction mixture.

Catalyst Pt1Sn3/SiO_2. The best fit of the spectra after the catalyst reduction at 220°C was obtained assuming only one Pt–Sn component. It had the IS of 2.19 mm s^{-1}, close to that of $PtSn_2$ (49). The subsequent reduction of the sample at 350°C led to the shift of the IS for the Pt–Sn alloy species to 1.81 mm s^{-1}, which is similar to that of PtSn phase (49). Simultaneously, another Sn-rich Pt–Sn alloy emerged, with the IS of 2.53 mm s^{-1}. This value is very close to that of β-Sn (2.58 mm s^{-1} (49)). Thus, the $PtSn(b_2)$ species might be identified even as unalloyed metallic Sn. Exposure of the reduced sample to the reaction mixture resulted in an increase in the IS value of the $PtSn(b_1)$ species from 1.81 to 2.18 mm s^{-1}, which is characteristic of $PtSn_2$ (49), in the disappearance of the Sn-rich $PtSn(b_2)$ alloy, and in the formation of a small fraction of a Pt-rich Pt–Sn alloy with the IS of 1.19 mm s^{-1} (diluted solution of Sn in Pt (49)). The RIs of the ionic Sn species were almost independent of the catalyst treatment.

The total spectral area related to the baseline significantly increased after reduction for all the catalysts studied (Table 4). This increase is assigned to the different recoilless fractions for the Sn(IV) species and Pt–Sn alloys, as well as to possible agglomeration of the Sn(IV) at elevated temperatures. The recoilless fraction for the bulk tin dioxide was found to be larger than that for the surface Sn(IV) ions (54).

DISCUSSION

Catalytic Performance

A common feature of Pt–Sn catalysts in a number of Pt-catalyzed reactions is a suppressed rate of deactivation and lower activity compared to those of pure Pt (10, 12, 14, 16–18, 20, 32, 47, 56–59). It has also been shown that a small addition of Sn to Pt, in fact, increases activity of the latter in hydrocarbon conversion reactions (14, 57–62). The present investigation showed that the reaction of hydrogen-assisted 1,2-dichloroethane dechlorination is not an exception. While the Pt/SiO_2 constantly deactivates with TOS (Fig. 1), the activity of Pt–Sn catalysts insignificantly decreases only during 1–2 h on stream, remaining constant thereafter (Fig. 2, Tables 2 and 3). In addition, activity of the Pt–Sn catalysts passes through a maximum as the Sn-to-Pt atomic ratio increases (Tables 2 and 3).

Another common feature of Pt–Sn catalysts is dramatically different selectivity of Pt in hydrocarbon conversion reactions upon the addition of Sn (10, 12–14, 18, 20, 32, 47, 55, 57, 58, 60, 62–64). The performance of the Pt–Sn/SiO_2 catalysts in 1,2-dichloroethane hydrodechlorination in terms of selectivity was consistent with the trends observed for hydrocarbon conversion reactions. The Pt/SiO_2 catalyzes the formation of ethane and monochloroethane with selectivities of 82–83% and 17–18%, respectively (Tables 2 and 3). The addition of Sn results in a gradual decrease of monochloroethane selectivity to 5% for the catalyst with the Pt/Sn ratio of 1. However, further decreasing the Pt/Sn ratio completely suppresses the monochloroethane pathway, and ethylene, for all practical purposes, is the sole reaction product for the Pt1Sn3/SiO_2 (Table 2 and 3).

Nevertheless, there is a fundamental difference between hydrocarbon conversion and dechlorination reactions catalyzed by Pt–Sn catalysts. Tin is inert with respect to activating the bonds in hydrocarbons; however, Sn as well as Pt catalyze the dissociation of C–Cl bonds in chlorocarbons. Thus, it is important to consider the interaction of each reactant with each metal site in order to develop an understanding of the relationship between catalyst microstructure and reactivity.

Catalyst Microstructure

It is well-known that various intermetallic Pt–Sn compounds exhibit different adsorptive properties toward H_2 and hydrocarbons which impacts catalytic performance (39, 55, 59, 61, 64–66). Based on the kinetics data for the 1,2-dichloroethane dechlorination (Tables 2 and 3), it is reasonable to suggest that the catalytic properties of Pt-rich Pt–Sn species (Pt/Sn > 1) are close to those of Pt, whereas the properties of Sn-rich Pt–Sn species (Pt/Sn ≤ 1) are quite different. Ethylene appears to form on the Sn-rich Pt–Sn species.

According to the Mössbauer spectroscopy data (Table 4), a fraction of Pt in all the Pt–Sn catalysts is incorporated into Sn-rich Pt–Sn species. However, the Pt1Sn1/SiO_2 exhibited no selectivity toward ethylene (Tables 2 and 3). These two results can be understood if one assumes that

(i) the Pt1Sn1/SiO_2 catalyst contains separate Pt_3Sn and $PtSn_4$ particles and (ii) the surface of the latter particles is enriched with Sn to the extent that metallic Sn completely covers the surface of the $PtSn_4$ species. In this case only the Pt_3Sn particles contribute to the macroscopic catalytic performance. It is worth noting that identification of β-Sn and $PtSn_4$ alloy by Mössbauer spectroscopy is very difficult when they coexist because their isomer shifts are similar (49); however, the β-Sn species would react stoichiometrically with the chlorohydrocarbon to form a Sn–Cl species that is completely inactive.

A characteristic feature of the Pt1Sn2/SiO_2 is that a significant fraction of Sn is incorporated into a Pt–Sn alloy with the stoichiometry of $Pt_\infty Sn$ (species Pt–Sn(a), Table 4). Similar to the pure Pt, this species would catalyze 1,2-dichloroethane dechlorination to form ethane. The fraction of the $Pt_\infty Sn$ species in the catalyst increased after 24 h on stream (Table 4), in parallel with an increase in ethylene selectivity in the $CH_2Cl–CH_2Cl + H_2$ reaction (Fig. 2, Tables 2 and 3). This shows that the impact of the $Pt_\infty Sn$ species on the catalytic behavior of the Pt1Sn2/SiO_2 decreased with TOS. It might be that, in addition to Pt–Sn alloy species, the reduced catalyst contained a fraction of unalloyed Pt. As the $CH_2Cl–CH_2Cl + H_2$ reaction proceeded, this Pt alloyed with Sn that had been in an oxidized state (the fraction of ionic Sn decreased with TOS, Table 4) to form an additional amount of the $Pt_\infty Sn$ species. At the same time the reaction mixture caused the surface enrichment of the Pt-rich Pt–Sn species with Sn, thereby making such particles selective toward ethylene. This process explains the transient behavior of the Pt1Sn2/SiO_2 in terms of ethylene selectivity (Fig. 2).

The further decrease in the Pt-to-Sn atomic ratio in the Pt–Sn catalysts resulted in the formation of the ethylene-selective $PtSn_2$ species after the reduction of the Pt1Sn3/SiO_2 at 220°C (Table 4). Surprisingly, the subsequent reduction of the same sample at 350°C caused the $PtSn_2$ to be transformed into the other ethylene-selective species, PtSn (species Pt–Sn(b_1), Table 4). Such a transformation can be understood if the bimetallic particles in the catalyst reduced at 220°C have a cherrylike structure, with the $PtSn_2$ alloy encompassing the unalloyed Pt. Otherwise, the catalyst would not be highly selective toward ethylene.

The mechanism to form such "cherrylike" particles may be the following. As platinum chlorides reduce readily, they reduce first to form metallic Pt particles. This Pt catalyzes the reduction of migrating Sn chloride species to form a Pt–Sn alloy starting from the surface of the Pt particles. The thickness of the Pt–Sn alloy is controlled by the rate of the bulk diffusion of Sn in Pt, in other words by temperature. The composition of the alloy depends on the transport of the Sn chloride species to the Pt particles. The transport, in turn, depends on the metal loading, Pt/Sn atomic ratio, and temperature as well. Increasing the temperature to 350°C during the second reduction accelerates the diffusion of Sn in Pt. This results in the dilution of the $PtSn_2$ with Pt to form PtSn. Concomitantly, a fraction of remote Sn chlorides reduces to the metal (species Pt–Sn(b_2), Table 4). Exposure of the reduced catalyst to the reaction mixture at 200°C leads to the redistribution of Sn moieties via the formation of mobile Sn chlorides. This resulted in the emergence of the $PtSn_2$ alloy as a dominant Pt–Sn species. Surface enrichment with Sn caused by the reaction mixture might be responsible for formation of a small fraction of the Pt-rich Pt–Sn alloy (species Pt–Sn(a), Table 4) located in the interior of the $PtSn_2$ alloy particles.

Unraveling the Role of Pt and Sn

To explain the advantageous role of tin in Pt–Sn catalysts, two mechanisms have been brought forward. The first is the "ensemble" or "geometric" effect. By forming a substitutional alloy at low concentrations or an intermetallic compound at higher concentration, tin separates platinum ensembles (reducing the number of or eliminating Pt-only threefold hollow sites) and maintains Pt in high dispersion (30, 39, 67). The second is the "ligand" or "electronic" effect. In this case, due to a partial charge transfer from Sn or due to the different electronic structure in Pt–Sn alloys, there is a modification of the platinum electron properties (12, 68–70). As a result, the presence of neighboring Sn atoms appears to modify the interaction of surface Pt atoms with adsorbed hydrogen and hydrocarbon species (23, 28, 39, 66, 70–73). For example, increased selectivity of supported Pt–Sn catalysts in paraffin dehydrogenation toward olefins was explained by lower heat of olefin adsorption on Pt–Sn alloys compared to that on pure Pt (17, 63). High selectivity of Pt–Sn/Al_2O_3 toward olefins in *n*-hexane conversion was assigned to the absence of sufficient hydrogen on the surface of the bimetallic catalyst (74, 75).

Indeed, the adsorption of H_2 on Pt at ambient temperature strongly decreases with increasing Sn content in both bulk Pt–Sn alloys and supported Pt–Sn catalysts (39, 76). A surface science study provided evidence that the dissociative H_2 adsorption is activated on the $Pt_3Sn(111)$ and $Pt_2Sn(111)$ surfaces (65). Nevertheless, this phenomenon may not be responsible for high selectivity of the Pt–Sn/SiO_2 toward ethylene in 1,2-dichloroethane dechlorination. It was shown that Sn can even increase the H_2 adsorption on Pt at elevated temperatures (76). In addition, a lack of H adatoms on the surface Pt–Sn species under reaction conditions would result in catalyst deactivation because of Cl poisoning. To this end, a significant decrease in the heat of olefin adsorption as Sn is added to Pt (38, 66) seems to be a most likely reason for the high olefin selectivity of the Pt–Sn/SiO_2 catalysts in the $CH_2Cl–CH_2Cl + H_2$ reaction.

Another mechanism to explain the role of Pt and Sn in Pt–Sn catalyst for the 1,2-dichloroethane dechlorination that cannot be disregarded *a priori* is that for the given

reaction Pt and Sn are responsible for different elementary steps. Namely, dissociation of 1,2-dichloroethane occurs on Sn sites. Because Sn is not capable of chemisorbing olefins, ethylene precursor, $\cdot CH_2–CH_2\cdot$ formed from $CH_2Cl–CH_2Cl$, immediately desorbs into the gas phase. Hydrogen activates on Pt and its surface diffusion to Sn is responsible for the scavenging of Cl atoms thereon.

CONCLUSION

Hydrogen-assisted 1,2-dichloroethane dechlorination has been investigated for silica-supported Pt and Pt–Sn catalysts at 200°C and atmospheric pressure. The Pt-to-Sn atomic ratio for the bimetallic catalysts was varied from 10 to 0.3. For the Pt/SiO_2-catalyzed reaction, 1,2-dichloroethane conversion constantly decreased with time to drop by one order of magnitude in 100 h on stream. Addition of Sn to Pt suppressed catalyst deactivation. Ethane and monochloroethane were the reaction products for the Pt and Pt–Sn catalysts with a Pt/Sn atomic ratio ≥ 1, with selectivity toward the latter progressively decreasing as the Pt/Sn ratio decreased. Dramatic change in product selectivity was observed when the Pt/Sn ratio became less than unity. Ethylene and ethane became the only reaction products with steady-state ethylene selectivity of 98% for the catalyst with a Pt/Sn atomic ratio of 0.3. According to an *in situ* Mössbauer spectroscopic study, a considerable fraction of Sn in ethylene-selective $Pt1Sn3/SiO_2$ and $Pt1Sn2/SiO_2$ and in unselective $Pt1Sn1/SiO_2$ catalysts formed Pt–Sn alloys, with the rest of Sn being present as Sn^{4+} and Sn^{2+}. Only a Sn-rich Pt–Sn alloy was in the $Pt1Sn3/SiO_2$ catalyst after reduction, while both Sn-rich and Pt-rich Pt–Sn alloy species were present in the $Pt1Sn1/SiO_2$ and $Pt1Sn2/SiO_2$ samples. It is suggested that Sn-rich Pt–Sn alloys such as $PtSn_4$, $PtSn_2$, and PtSn are responsible for the formation of ethylene in the $CH_2ClCH_2Cl + H_2$ reaction. The different catalytic performances of $Pt1Sn2/SiO_2$ and $Pt1Sn1/SiO_2$ catalysts is explained by the different catalysts' microstructure. For the ethylene-selective $Pt1Sn2/SiO_2$, the Sn-rich Pt–Sn alloy phase would encompass the Pt–rich one, forming a cherrylike structure, with the interior being a Pt-rich Pt–Sn alloy. For the ethylene-unselective $Pt1Sn1/SiO_2$ both Pt-rich and Sn-rich alloy phases are exposed to the reaction mixture. The surface enrichment of the Sn-rich Pt–Sn alloy with Sn resulting in a complete blocking of the surface with Sn was suggested to be responsible for the absence of ethylene as a reaction product in this case.

ACKNOWLEDGMENT

Financial support from the Department of Energy–Basic Energy Sciences (DE-FG02-95ER14539) is gratefully acknowledged.

REFERENCES

1. Vadlamannati, L. S., Luebke, D. R., Kovalchuk, V. I., and d'Itri, J. L., *Appl. Catal. B* **35**, 211 (2002).
2. Vadlamannati, L. S., Luebke, D. R., Kovalchuk, V. I., and d'Itri, J. L., *Stud. Surf. Sci. Catal.* **130**, 233 (2000).
3. Vadlamannati, L. S., Kovalchuk, V. I., and d'Itri, J. L., *Catal. Lett*. **58**, 173 (1999).
4. Heinrichs, B., Schoebrechts, J.-P., and Pirard, J.-P., *J. Catal*. **200**, 309 (2001).
5. Heinrichs, B., Schoebrechts, J.-P., and Pirard, J.-P., *Stud. Surf. Sci. Catal*. **130**, 2015 (2000).
6. Heinrichs, B., Delhez, P., Schoebrechts, J.-P., and Pirard, J.-P., *Stud. Surf. Sci. Catal*. **118**, 707 (1998).
7. Heinrichs, B., Delhez, P., Schoebrechts, J.-P., and Pirard, J.-P., *J. Catal*. **172**, 322 (1997).
8. Early, K. O., Rhodes, W. D., Kovalchuk, V. I., and d'Itri, J. L., *Appl. Catal. B* **26**, 257 (2000).
9. Davis, B. H., *J. Catal*. **46**, 348 (1977).
10. Karpinski, Z., and Clarke, J. K. A., *J. Chem. Soc. Faraday Trans. 2* **71**, 893 (1975).
11. Szabo, G. L., *Stud. Surf. Sci. Catal.* **11**, 349 (1982).
12. Burch, R., and Garla, L. C., *J. Catal*. **71**, 360 (1981).
13. Kuznetsov, B. N., Duplyakin, V. K., Koval'chuk, V. I., Ryndin, Yu. A., and Belyi, A. S., *Kinet.Catal.* **22**, 1183 (1982).
14. Coq, B., and Figueras, F., *J. Catal*. **85**, 197 (1984).
15. Kappenstein, C., Guérin, M., Lázár, K., Matusek, K., and Paál, Z., *J. Chem. Soc. Faraday Trans*. **94**, 2463 (1998).
16. Bariås, O. A., Holmen, A., and Blekkan, E. A., *J. Catal*. **158**, 1 (1996).
17. Cortright, R. D., and Dumesic, J. A., *J. Catal*. **148**, 771 (1994).
18. Davis, B. H., Westfall, G. A., Watkins, J., and Pezzanite, J., Jr., *J. Catal*. **42**, 247 (1976).
19. Bacaud, R., Bussiere, P., Figueras, F., and Mathieu, J. P., *in* "Preparation of Catalysts" (B. Delmon, P. A. Jacobs, and G. Poncelet, Eds.), p. 509. Elsevier, Amsterdam, 1976.
20. Ryndin, Yu. A., Lorent, J., Kuznetsov, B. N., Koval'chuk, V. I., Pentenero, A., and Yermakov, Yu. I., *Kinet. Catal.* **22**, 513 (1982).
21. Kern-Tálas, E., Hegedüs, M., Göbölös, S., Szedlacsek, P., and Margitfalvi, J., *Stud. Surf. Sci. Catal*. **31**, 689 (1987).
22. Llorca, J., Homs, H., Fierro, J.-L. G., Sales, J., and Ramírez de la Piscina, P., *J. Catal*. **166**, 44 (1997).
23. Balakrishnan, K., and Schwank, J., *J. Catal*. **127**, 287 (1991).
24. Balakrishnan, K., and Schwank, J., *J. Catal*. **138**, 491 (1992).
25. Barbier, J., *Appl. Catal*. **23**, 225 (1986).
26. Bariås, O. A., Holmen, A., and Blekkan, E. A., *in* "Catalyst Deactivation" (B. Delmon and G. F. Froment, Eds.), p. 519. Elsevier Science B. V., New York, 1994.
27. Lane, G. S., Modica, F. S., and Miller, J. T., *J. Catal*. **129**, 145 (1991).
28. Lieske, H., Sárkány, A., and Völter, J., *Appl. Catal*. **30**, 69 (1987).
29. Lin, L., Zhang, T., Zang, J., and Xu, Z., *Appl. Catal*. **67**, 11 (1990).
30. Meitzner, G., Via, G. H., Lytle, F. W., Fung, S. C., and Sinfelt, J. H., *J. Phys. Chem*. **92**, 2925 (1988).
31. Merlen, E., Beccat, P., Bertolini, J. C., Delichére, P., Zanier, N., and Didillon, B., *J. Catal*. **159**, 178 (1996).
32. Natal-Santiago, M. A., Podkolzin, S. G., Cortright, R. D., and Dumesic, J. A., *Catal. Lett*. **45**, 155 (1997).
33. Passos, F. B., Schmal, M., and Vannice, M. A., *J. Catal*. **160**, 106 (1996).
34. Passos, F. B., Schmal, M., and Vannice, M. A., *J. Catal*. **160**, 118 (1996).
35. Schwank, J., Balakrishnan, K., and Sachdev, A., *Stud. Surf. Sci. Catal*. **75**, 905 (1983).
36. Sexton, B. A., Hughes, A. E., and Foger, K., *J. Catal*. **88**, 466 (1984).
37. Sharma, S. B., Miller, J. T., and Dumesic, J. A., *J. Catal*. **148**, 198 (1994).
38. Shen, J., Hill, J. M., Watwe, R. M., Spiewak, B. E., and Dumesic, J. A., *J. Phys. Chem. B*. **103**, 3923 (1999).
39. Verbeek, H., and Sachtler, W. M. H., *J. Catal*. **42**, 257 (1976).

40. Massalski, T. B., Okamoto, H., Subramanian, P. R., and Kacprzak, L., Eds., "Binary Alloy Phase Diagrams." ASM International, Materials Park, OH, 1990.
41. Cotton, F. A., and Wilkinson, G., "Advanced Inorganic Chemistry." Wiley, New York, 1988.
42. Lindsey, R. V., Jr., Parshall, G. W., and Stolberg, U. G., *Inorg. Chem.* **5**, 109 (1966).
43. Young, J. F., Gillard, R. D., and Wilkinson, G., *J. Chem. Soc.* **12**, 5176 (1964).
44. Lázár, K., *Struct. Chem.* **2**, 245 (1991).
45. Parish, R. V., *in* "Mössbauer Spectroscopy Applied to Inorganic Chemistry" (G. J. Long, Ed.), Vol. 1, p. 527. Plenum, New York, 1984.
46. Li, Y.-X., Klabunde, K. J., and Davis, B. H., *J. Catal.* **128**, 1 (1991).
47. Bacaud, R., Bussière, P., and Figueres, F., *J. Catal.* **69**, 339 (1981).
48. Hobson, M. C., Jr., Goresh, S. L., and Khare, G. P., *J. Catal.* **142**, 641 (1993).
49. Charlton, J. S., Cordey-Hayes, M., and Harris, I. R., *J. Less-Common Met.* **20**, 105 (1970).
50. Greenwood, N. N., and Gibb, T. C., "Mössbauer Spectroscopy." Chapman & Hall, London, 1971.
51. Kuznetsov, V. I., Belyi, A. S., Yurchenko, E. N., Smolikov, M. D., Protasova, M. T., Zatolokina, E. V., and Duplyakin, V. K., *J. Catal.* **99**, 159 (1986).
52. Hayes, M. C., *in* "Chemical Applications of Mössbauer Spectroscopy" (V. I. Goldanskii and R. H. Herber, Eds.), p. 314. Academic Press, New York, 1968.
53. Bryukhanov, V. A., Delyagin, N. N., Kuz'min, R. N., and Shpinel', V. S., *Sov. Phys. JETP* **19**, 1344 (1964).
54. Lázár, K., Rhodes, W. D., Borbáth, I., Hegedüs, M., and Margitfalvi, J. L., *Hyperfine Interact.*, in press.
55. Dautzenberg, F. M., Helle, J. N., Biloen, P., and Sachtler, W. M. H., *J. Catal.* **63**, 119 (1980).
56. Völter, J., Lietz, G., Uhlemann, M., and Hermann, M., *J. Catal.* **68**, 42 (1981).
57. Poltarzewski, Z., Galvagno, S., Pietropaolo, R., and Staiti, P., *J. Catal.* **102**, 190 (1986).
58. Coq, B., and Figueras, F., *J. Mol. Catal.* **25**, 87 (1994).
59. Xu, C., and Koel, B. E., *Surf. Sci.* **304**, 249 (1994).
60. Coq, B., Tijani, A., and Figuéras, F., *J. Mol. Catal.* **71**, 317 (1992).
61. Szanyi, J., Anderson, S., and Paffett, M. T., *J. Catal.* **149**, 438 (1994).
62. Margitfalvi, J. L., Borbáth, I., and Tompos, A., *Stud. Surf. Sci. Catal.* **118**, 195 (1998).
63. Yokoyama, C., Bharadwaj, S. S., and Schmidt, L. D., *Catal. Lett.* **38**, 181 (1996).
64. Peck, J. W., and Koel, B. E., *J. Am. Chem. Soc.* **118**, 2708 (1996).
65. Paffett, M. T., Gebhart, S. C., Windham, R. G., and Koel, B. E., *J. Phys. Chem.* **94**, 6831 (1990).
66. Tsai, Y.-L., Xu, C., and Koel, B. E., *Surf. Sci.* **385**, 37 (1997).
67. Li, Y. X., and Klabunde, K. J., *J. Catal.* **126**, 173 (1990).
68. Burch, R., *J. Catal.* **71**, 348 (1981).
69. Bariås, O. A., Holmen, A., and Blekkan, E. A., *Catal. Today* **24**, 361 (1995).
70. Palazov, A., Bonev, Ch., Shopov, D., Lietz, G., Sárkány, A., and Völter, J., *J. Catal.* **103**, 249 (1987).
71. Paffett, M. T., Gebhard, S. C., Windham, R. G., and Koel, B. E., *Surface Sci.* **223**, 449 (1989).
72. de Miguel, S., Castro, A., Scelza, O., Fierro, J. L. G., and Soria, J., *Catal. Lett.* **36**, 201 (1996).
73. Park, Y.-K., Ribeiro, F. H., and Somorjai, G. A., *J. Catal.* **178**, 66 (1998).
74. Paál, Z., Xu, X. L., Paál-Lukács, J., Vogel, W., Muhler, M., and Schlögl, R., *J. Catal.* **152**, 252 (1995).
75. Sárkány, A., *J. Chem. Soc. Faraday Trans. 1* **85**, 1523 (1989).
76. Lieske, H., and Völter, J., *J. Catal.* **90**, 96 (1984).